Ascent Rates of Rhyolitic Magma at the Onset of Supervolcanic Eruptions

Madison L. Myers[1*], Paul J. Wallace[1] and Colin J. N. Wilson[2]

1. Department of Geological Sciences, 1272 University of Oregon, Eugene OR 97403-1272 2. SGESS, Victoria University, Wellington, NZ

*Questions? Email: mmyers3@uoregon.edu

Meet the Volcanoes: Background

Huckleberry Ridge Tuff , Yellowstone (2.1 Ma, 2,500 km^3)

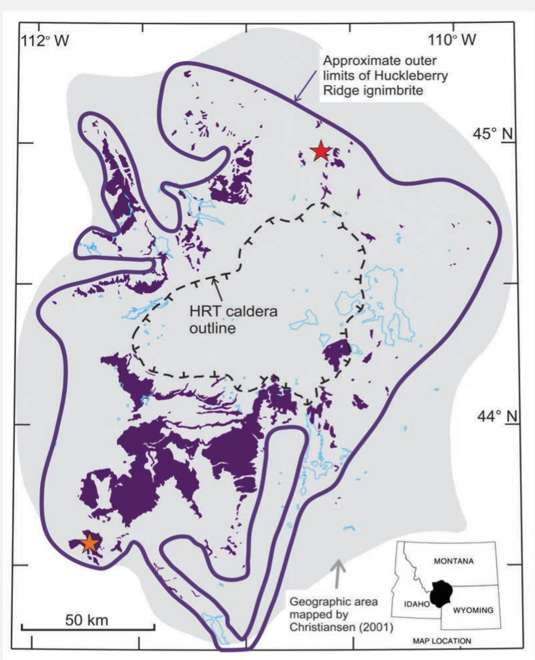

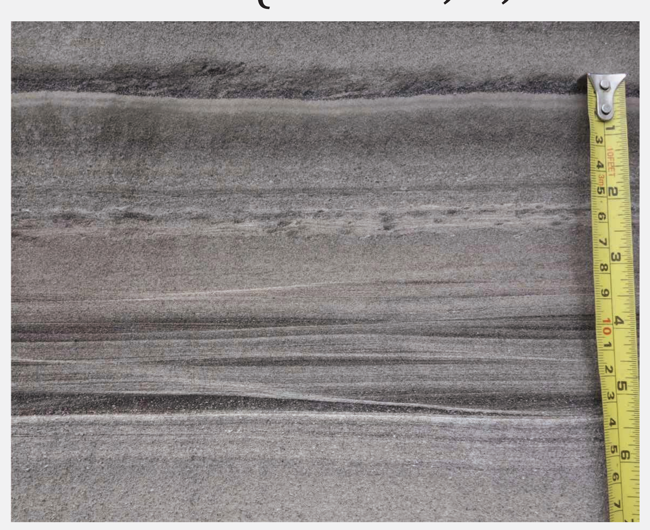

Fig. 1: (left) Outline map of the area covered by ignimbrite of the Huckleberry Ridge Tuff. The geographical area mapped [1] is shown by gray shading, purple areas represent outcrops of the ignimbrite, and the purple line represents the approximate outer limits of the ignimbrite. (above) Photo of the reworking observed in the first 0.5 meters of the Huckleberry Ridge fall deposit (red star).

The fine-grained ash to fine lapilli fallout deposit at the base of the Huckleberry Ridge Tuff preserves evidence for intrafall reworking, observed as layers of cross-bedding, normal grading, and rain interaction (Fig. 1). Each layer is interpreted to represent a time break on the order of days [2,3].

Bishop Tuff (0.76 Ma, 650 km^3)

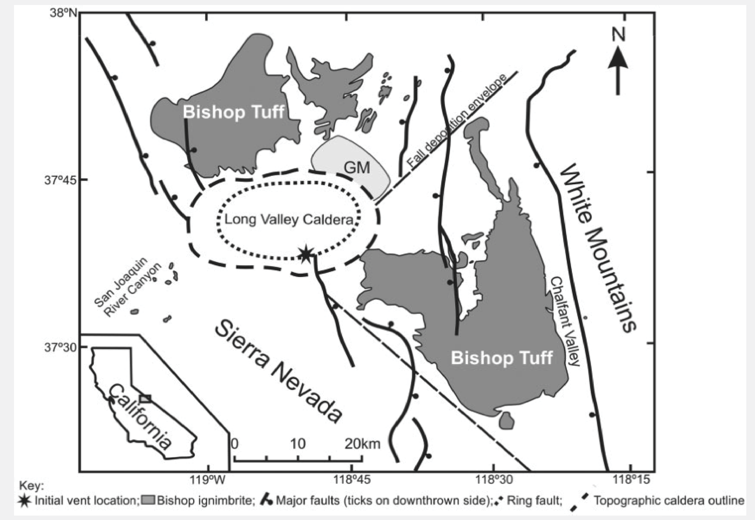

Fig. 2: (left) The basal fall deposit becomes interbedded with pyroclastic material in its upper portion, preserved beautifully in the Chalfont Quarry. (right) Regional map of the Long Valley Caldera [4], where star represents the opening vent location for the Bishop Tuff eruption.

The rapid and continuous transition observed between fall layers and flow initiation (Fig. 4) suggests that the Bishop Tuff represents our best example of a continuous caldera forming eruption, where the entire deposit from start to finish is inferred to have occurred over six days [4].

Oruanui, Taupo NZ (26.5 ka, 530 km^3)

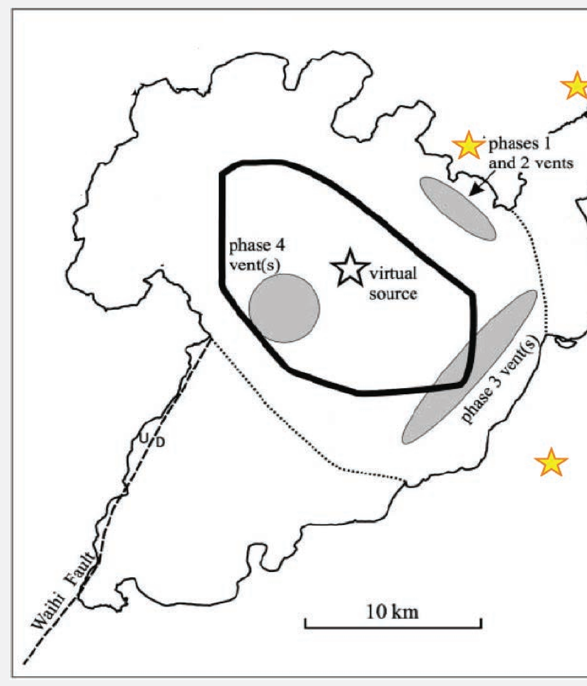

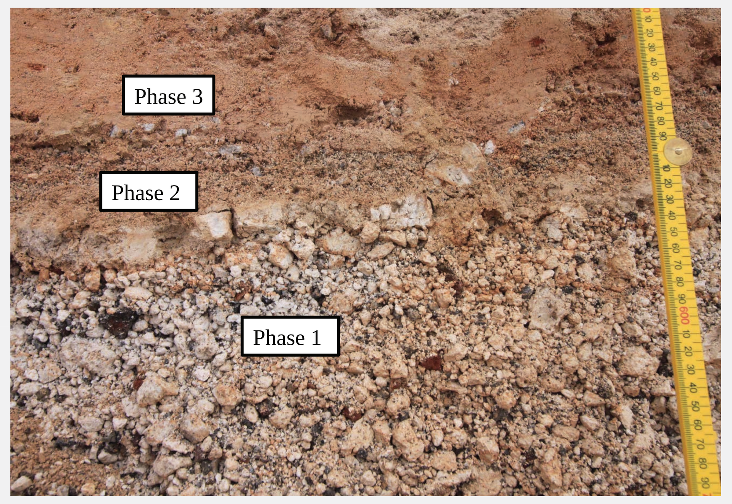

Fig. 3: (left) Generalize outline of the Oruanui caldera. Stars represent sampling sites from this study. Grey ovals display the vent locations for the first four phases of the eruption [5]. (right) Photo of a field location where all three phases are present.

The whole of the Oruanui eruption consists of ten phases, where time breaks exist between five of the transitions [5]. The most defined time gap is between phase 1 and 2, representing an eruption break on the order of days to weeks [5]. These first two phases are also associated with a rifting event that facilitated the lateral injection of a biotite-bearing foreign magma into the eruption [6].

Methods for Calculating Timescales

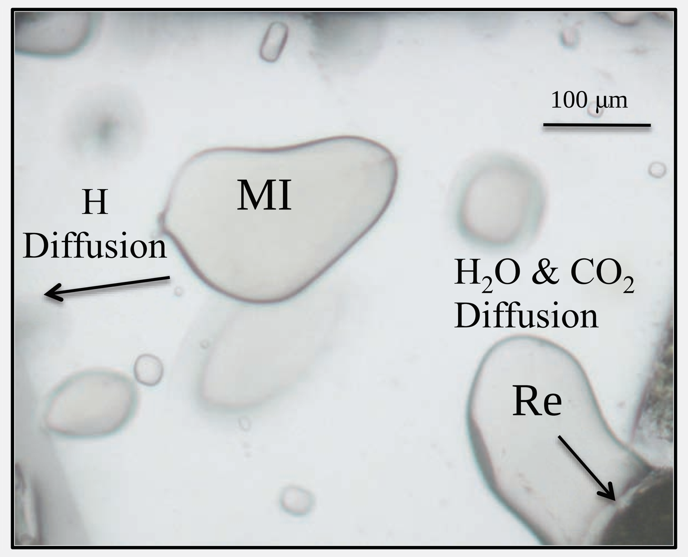

Fig. 4: Photo of a quartz-hosted melt inclusion (MI) and reentrant (RE).

- H diffusion from an enclosed melt inclusion (MI) through quartz to the external melt can occur on timescales of days

-H_2O and CO_2 gradients formed in reentrants (RE) during final ascent; timescales of hours.

<u>FTIR (Fourier Transform Infrared Spectroscopy)</u>

H_2O & CO_2 concentrations were measured on doubly intersected inclusions using the FTIR.

Timescales of Initial Ascent

In each horizon from the Huckleberry Ridge and Oruanui deposits there is a wide range of H_2O concentrations in sealed MIs, but restricted ranges in CO_2. In contrast to the wide range of H_2O, trace elements in the MIs from each sample vary by less than a factor of two. These patterns are best explained by diffusive loss of H from MIs during ascent. The highest H_2O values reflect the magma H_2O content at the storage depth prior to eruption, and lower values reflect variable diffusive losses [3].

Calculating the timescale of diffusive loss of H_2O from each MI through the quartz host requires estimates of:

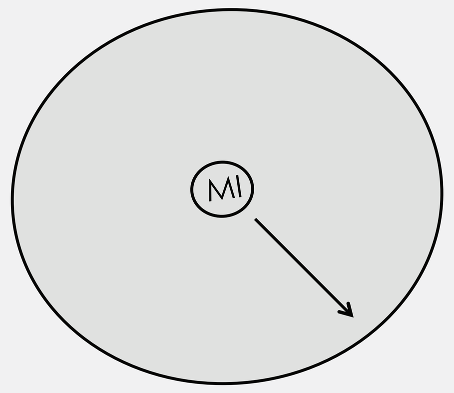

(1) the diffusion coefficient of H in quartz (10^{-11} m^2/s), based on the experiemental data by [7]

(2) the H_2O partition coefficient between quartz and melt (0.001; [8]),

(3) the initial MI H_2O concentration, estimated using trace element relationships or the highest concentration from each layer.

(4) the external H_2O concentration, based on the inner most reentrant concentration.

Fig. 5: The diffusion model assumes a perfectly spherical MI in the center of a spherical phenocryst [8,9]. In our model calculations, we chose the 'radius' of the quartz phenocryst to be the minimum distance (rather than the average) between the actual MI and the crystal rim (measured in 2D section).

Timescales of Final Ascent

During ascent, pressure dependent volatiles, such as H_2O and CO_2, will exsolve and form gas bubbles. As reentrants are in continued diffusional contact with the surrounding melt, volatile gradients form in the reentrants during this time as they strive to diffusively reequilibrate with the changing external melt. Using a numerical diffusion model, the decompression rate creates a profile that best fits the measured profile can be determine [3,10,11,12].

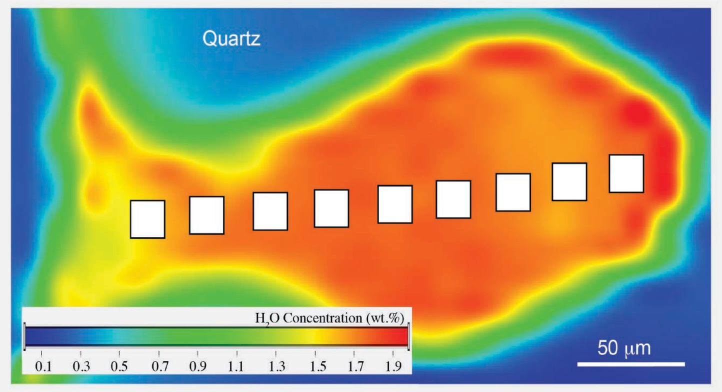

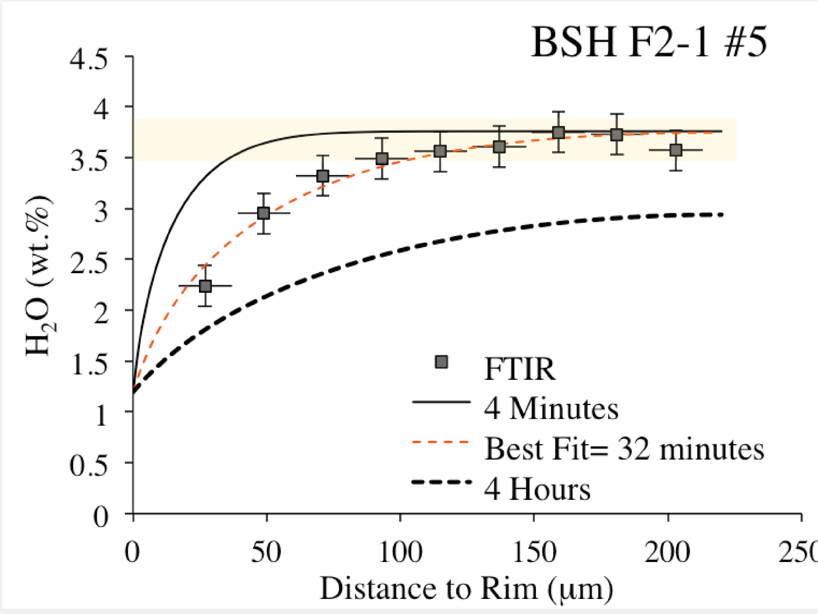

Fig. 6: (left) H_2O concentration map for a 200-µm-long reentrant from the Huckleberry Ridge. The nine white boxes represent the FTIR aperture locations (20 x 20 µm). (right) Measured H_2O profile for a Bishop reentrant, with modeled profiles overlain. The best fit profile for this sample is shown as the red dashed line, which represents an ascent time of 32 minutes.

<u>ACKNOWLEDGEMENTS</u>

Research supported by the 2013 Jack Kleinman Grant for Volcano Research, previous support by Marsden Grant VUW0813 and NSF Grant EAR-1524824.

What we've learned

Huckleberry Ridge

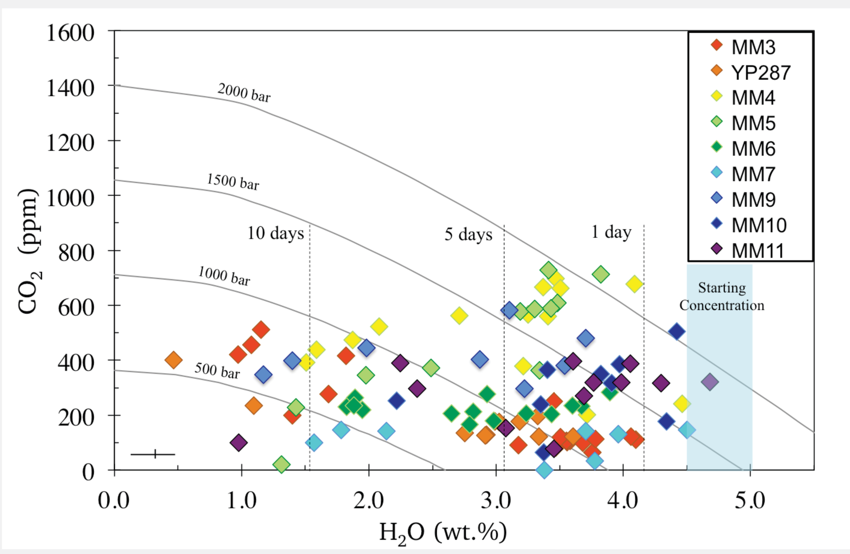

Oruanui

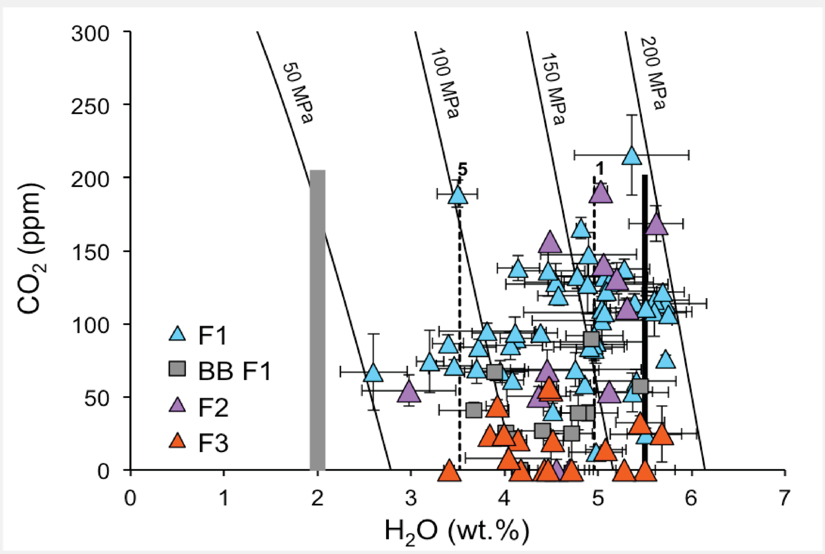

Fig. 7: Measured H_2O concentrations of fully enclosed inclusions as a function of layer. The dashed lines represent the concentration of H_2O for an average inclusion of 100 µm after a specified time of diffusive loss in a depressurized melt. For the Huckleberry Ridge this concentration is set at 1 wt.% H_2O, whereas in the Oruanui this external concentration is set at 2 wt.% H_2O. The initial concentration for all MIs lies within the shaded field (HRT~4.5 wt.%, Oruanui ~5.5 wt.%). Inclusions containing H_2O concentrations close to the shaded region imply ascent timescales of less than 12 hours and thus most closely represent pre-ascent storage conditions. In contrast, inclusions with low H_2O require loss to the external melt at lower pressures for 5 days in the Oruanui, and up to 10 days in the Huckleberry.

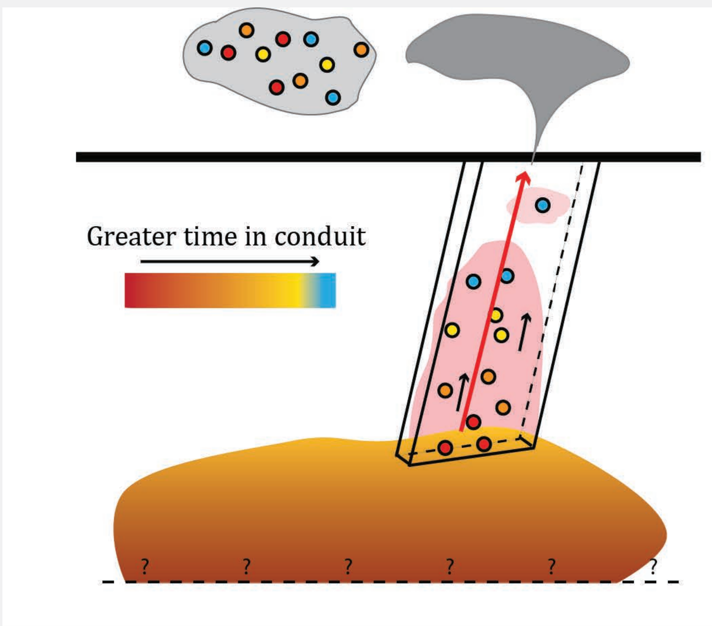

Scatter in H_2O concentrations in quartz-hosted inclusions from any single fall layer or pumice clasts suggests that individual grains that initially experienced different decompression histories were erupted simultaneously during a final explosive phase (Fig. 8).

Fig. 8: (left) Simplified skematic for the ascent history preserved by single depositional layers or pumices that contain a large degree of scatter in H_2O.

Fig. 9: (below) Each diamond represents the ascent rate modeled for an individual reentrant, positioned according to their relative stratigraphic location. The bottom of the diagram represents the earliest erupted material. Diamonds containing an X represent reentrants that lacked measurable CO_2, meaning ascent rates were constrained by modeling H_2O solely.

Ascent rate (m/s) for all three caldera forming eruptions overlap (Fig. 9), suggesting that any initial, sluggish behavior that may have occurred is not preserved in volatile gradients.

Overall, there are a higher number of faster ascent rates higher in the stratigraphy for the Bishop and Huckleberry Ridge tuffs.

In the Oruanui eruption, the first two phases are associated with slow ascent rates. Phase 3 jumps an order of magnitude. This shift is also associated with the change from a single vent to an elongate source and higher eruptive flux (Fig. 3).

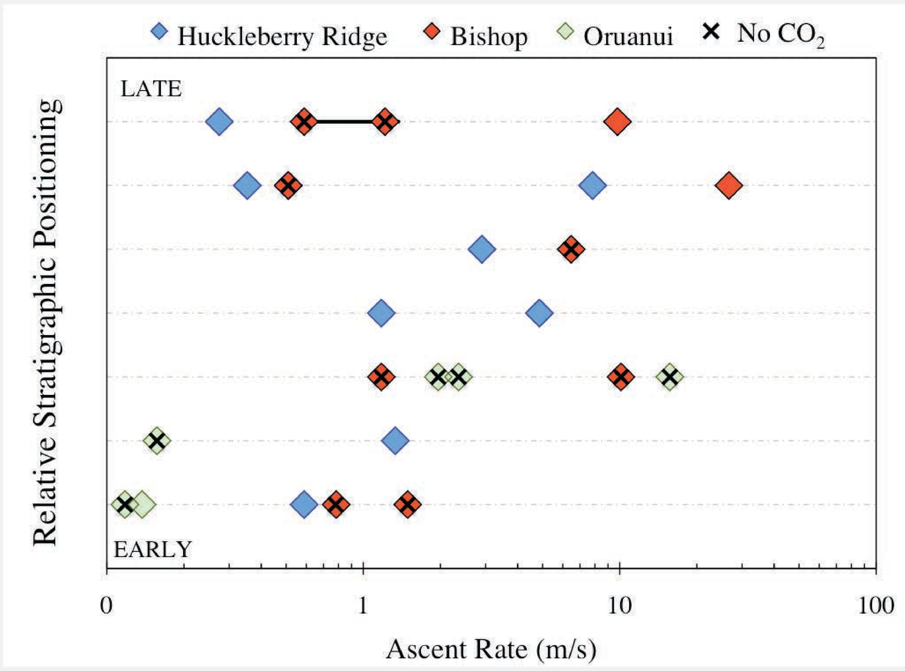

Take Home Points

> In contrast to the <1-3 hour ascent times calculated from reentrants, variable diffusive loss of H from enclosed inclusions provides evidence for highly variable decompression (<12 hours to 5-7 days) for quartz from single layers/pumices.

> Scatter in inclusions from both the Oruanui and Huckleberry Ridge suggest sluggish initiation, perhaps indicative of low overpressure in the system. Evidence for an external control facilitating movement towards the surface?

> Reentrants may be able to inform on conduit opening processes/evolution.

References: [1] Christiansen (2001) The Quaternary and Pliocene Yellowstone Plateau volcanic field of Wyoming, Idaho, and Montana. U.S. Geol. Surv. Prof. Pap. 729-G, G1-G143; [2] Wilson (2009) AGU, #V23C-2085; [3] Myers et al. (2016) Prolonged ascent and episodic venting of discrete magma batches at the onset of the Huckleberry Ridge supereruption Yellowstone. Earth Planet. Sci. Lett 451, 285-297. [4] Wilson, C.J.N., Hildreth, W. (1997). The Bishop Tuff: new insights from eruptive stratigraphy. J. Geol. 105, 407-439. [5] Wilson (2001) The 26.5 ka Oruanui eruption, New Zealand: an introduction and overview. J. Volcanol. Geotherm. Res. 112, 132-174; [6] Allan et al. (2012) The invisible hand: tectonic triggering and modulation of a rhyolitic supereruption. Geology 40, 563-566. [7] Severs et al. (2007) Experimental determination of H_2O loss from melt inclusions during laboratory heating: evidence from Raman spectroscopy. Chem. Geol. 237, 358-371; [8] Qin (1992) Disequilibrium partial melting model and its implications for trace element fractionations during mantle melting. Earth Planet. Sci. Lett. 112, 75-90.; [9] Cottrell et al. (2002) Consequences of diffusive reequilibration for the interpretation of melt inclusions. Geochem. Geophys. Geosyst. 3, 1026; [10] Liu et al. (2007) Melt pockets in phenocrysts and decompression rates of silicic magmas before fragmentation. J. Geophys. Res. 112, B06204; [11] Humphreys et al. (2008) Magma ascent rates in explosive eruptions: constraints from H_2O diffusion in melt inclusions. Earth Planet. Sci. Lett. 270, 25-40; [12] Lloyd et al. (2014) NanoSIMS results from olivine-hosted melt embayments: magma ascent rate during explosive basaltic eruptions. J. Volcanol. Geotherm. Res. 283, 1-18;